A NUMERICAL OPTIMAL CONTROL APPROACH TO THE DESIGN OF AN OPTICAL FIBRE-BASED EVANESCENT FIELD SENSOR. ⋆

Peter M. Dower* **Peter M. Farrell*** **Brant C. Gibson****

* *Department of Electrical and Electronic Engineering*
The University of Melbourne, Australia
** *Department of Physics*
The University of Melbourne, Australia

Abstract: This paper presents an application of numerical optimization via dynamic programming in the design of a refractive index profile for an optical fibre-based evanescent field sensor. The designed sensor delivers approximately 15% of the total propagating electromagnetic field power to the surrounding environment for sensing purposes, representing a substantial improvement over previous ad-hoc designs delivering at most 9% (Gibson *et al.*, 2001).

Keywords: Dynamic programming, optimal control, evanescent field power maximization, refractive index profile, optical fibre sensor design, implicit Markov chain approximation method.

1. INTRODUCTION

Evanescent field spectroscopy is proving to be a viable and useful mechanism for the optical sensing of chemicals, toxins, gases and other species (Sutherland *et al.*, 1984; Anderson *et al.*, 1994; Hale and Payne, 1994; Kumar *et al.*, 2002; Helmers *et al.*, 1996; Singh and Gupta, 1995; John *et al.*, 2002; Preejith *et al.*, 2003). Such sensors exploit the interaction between guided modes of electromagnetic radiation propagating through and around the sensing device (in this case, an optical fibre), and the surrounding environment in which the species resides. Of fundamental importance in such a sensing setup is the proportion of the total guided field power contained in the evanescent field. By increasing this relative evanescent field power, the gain of the sensor can be improved. As the evanescent field is determined by the refractive index profile of the sensor and the surrounding environment, design of the sensor refractive index profile is critical. Typically, this profile has been selected in an ad-hoc way (Gibson *et al.*, 2001) by computing the evanescent field power for a set of different profiles and choosing the maximizer from that set. Clearly this is a suboptimal approach.

This paper presents a rigorous and explicit solution to a specific refractive index profile design problem, based on the results of (Dower *et al.*, 2004).

2. AN OPTICAL WAVEGUIDE MODEL

2.1 Separated scalar wave equation

We consider the propagation of electromagnetic radiation through an axially symmetric translationally invariant optical fibre waveguide structure.

⋆ This research was partially supported by the Australian Research Council.

Weak guidance (Snyder and Love, 1983) is a phenomenon that arises in optical waveguides when the range of refractive indices available within the fibre structure is relatively narrow. The effect of this approximation is to significantly simplify the optical waveguide model required.

Assumption (WG): The weak guidance approximation (Snyder and Love, 1983) holds.

Theorem 2.1. (Snyder and Love, 1983) Suppose that assumption **(WG)** holds. Then, an axially symmetric translationally invariant optical waveguide can be modelled via the following separated scalar wave equation (SSWE):

$$0 = \Gamma_\Phi \Phi_l(\phi), \tag{1}$$
$$0 = \tilde{\Gamma}_F F_{l,\beta,n}(s), \tag{2}$$

where $s := \frac{r}{R}$ defines the normalized radial coordinate, with R the radius of the fibre structure, and Γ_Φ and $\tilde{\Gamma}_F$ are the ordinary differential operators

$$\Gamma_\Phi := \frac{d^2}{d\phi^2} + l^2$$
$$\tilde{\Gamma}_F := \frac{d^2}{ds^2} + \frac{1}{s}\frac{d}{ds} + k^2R^2[n(s)]^2 - \frac{l^2}{s^2} - \beta^2R^2,$$

where $k = \frac{2\pi}{\lambda}$ is the wave number, λ is the wavelength, β is the group velocity and R is the fibre radius. The subscript notation $F_{l,\beta,n}$, Φ_l denotes the dependence of both the radial and angular components of the transverse field on the choice of separation parameter l. The total transverse component of the electric field is then $\psi(s,\phi) := F_{l,\beta,n}(s)\Phi_l(\phi)$.

2.2 Boundary conditions

The boundary conditions for (1) and (2) follow from Assumption **(FD)**, and state that

$$\Phi_l(0) = \Phi_l(2\pi),\ \frac{d\Phi_l}{d\phi}(0) = \frac{d\Phi_l}{d\phi}(2\pi) \tag{3}$$
$$lF_{l,\beta,n}(0) = 0,\ \frac{dF_{l,\beta,n}}{ds}(0) = 0 \tag{4}$$

for all $l \in \mathbf{Z}$. Boundary condition (3) restricts l to integer values, thereby defining a modal parameter. Additional boundary conditions arise when the field power is restricted to be finite. In that case,

$$\lim_{s\to\infty} F_{l,\beta,n}(s) = 0,\ \lim_{s\to\infty} \frac{dF_{l,\beta,n}}{ds}(s) = 0 \tag{5}$$

for all $l \in \mathbf{Z}$. In this paper, all boundary conditions (3), (4) and (5) apply.

2.3 State space representation

A state space representation for SSWE (2) will motivate the definition of another equivalent (and easier to solve) evanescent field maximization problem. To this end, define the state vector

$$x(s) := \begin{bmatrix} x_1(s) \\ x_2(s) \end{bmatrix} = \begin{bmatrix} F_{l,\beta,n}(s) \\ \frac{dF_{l,\beta,n}}{ds}(s) \end{bmatrix}. \tag{6}$$

Applying to SSWE (2) yields the state equation

$$\dot{x}(s) = f(s, x(s), u(s)) \tag{7}$$

where

$$f(s,x,u) := \left[\begin{array}{c|c} 0 & 1 \\ \hline \frac{l^2}{s^2} - u & -\frac{1}{s} \end{array}\right] x,$$
$$u := k^2R^2[n(s)]^2 - \beta^2R^2, \tag{8}$$

with trajectory $x(\cdot)$ initialized at the fibre / environment interface,

$$\begin{bmatrix} F_{l,\beta,n}(1) \\ \frac{dF_{l,\beta,n}}{ds}(1) \end{bmatrix} = \begin{bmatrix} x_1(1) \\ x_2(1) \end{bmatrix} = x_1 \in \mathbf{R}^2. \tag{9}$$

2.4 The evanescent field

The evanescent field describes the solution of SSWE (2) in the environment surrounding the fibre, that is, for $s \geq 1$. For general RIPs, this solution is difficult to determine, requiring the application of numerical methods in most cases. However, in many sensing environments, the RI is approximately constant, motivating the following assumption.

Assumption (E): The refractive index $n_e(\cdot) \in \mathcal{N}_0[1,\infty)$ of the environment surrounding the fibre sensor is constant. That is, $n_e(s) \equiv n_e \in \mathbf{R}_{\geq 0}$ for all $s \in [1,\infty)$.

Assumption **(E)** admits a well-known characterization of the general solution of SSWE (2), as per (Agrawal, 2001), (Snyder and Love, 1983).

Theorem 2.2. Fix $l \in \mathbf{Z}$, $\beta, n_e \in \mathbf{R}_{\geq 0}$ and suppose that assumption **(E)** holds. Then, the general solution of SSWE (2) for $s \geq 1$ (that is, in the environment surrounding the fibre structure) is

$$\begin{aligned} F_{l,\beta,n_e}(s) = {} & C_{l,\beta,n_e} K_l(W_{\beta,n_e}s) \\ & + D_{l,\beta,n_e} N_l(W_{\beta,n_e}s), \end{aligned} \tag{10}$$

where C_{l,β,n_e}, D_{l,β,n_e}, $W_{l,\beta} \in \mathbf{R}$ are constants,

$$W_{\beta,n_e} := kR\sqrt{n_{eff}^2 - n_e^2}, \quad n_{eff} := \frac{\beta}{k}, \tag{11}$$

and K_l, N_l are respectively an order l modified Bessel function and an order l Neumann function.

Note that $W_{\beta,n_e} \in \mathbf{R}$ as $n_{eff} > n_e$. Furthermore, the following properties of K_l and N_l hold (see (Agrawal, 2001)):

$$\begin{aligned} \lim_{s\to\infty} |K_l(s)| = 0, \quad \liminf_{s\to\infty} |N_l(s)| = \infty, \\ \lim_{s\to\infty} \left|\frac{dK_l}{ds}(s)\right| = 0, \ \liminf_{s\to\infty} \left|\frac{dN_l}{ds}(s)\right| = \infty. \end{aligned} \tag{12}$$

Corollary 2.3. Fix l, β, $n_e \in \mathbf{R}_{\geq 0}$ and suppose assumption **(E)** holds. Given a solution F of the SSWE (2), the following statements are equivalent:

(1) F is of the form (10) with $D_{l,\beta,n_e} = 0$.
(2) Boundary condition (5) holds.

2.5 Finite evanescent field power

The power in the transverse electric field $\psi(s,\cdot)$ for normalized radii in the range $s \in [s_1, s_2)$ is proportional to

$$\hat{P}(s_1, s_2; \psi) := \underbrace{\int_{s_1}^{s_2} sF_{l,\beta,n}(s)^2 \, ds}_{=:P(s_1,s_2;F_{l,\beta,n})} \underbrace{\int_0^{2\pi} \Phi_l(\phi)^2 \, d\phi}_{=:Q(\Phi_l)} \tag{13}$$

where the field amplitude $F_{l,\beta,n}(\cdot)$ is a solution to the boundary value problem (2), (4), (5), whilst the angular dependence $\Phi_l(\cdot)$ is a solution of the SSWE (1), (3). Note that the angular dependence can be calculated explicitly and is always finite. This motivates the following more general assumption.

Assumption (FP): The evanescent field power is finite.

Theorem 2.4. Fix l, β, $n_e \in \mathbf{R}_{\geq 0}$ and suppose that assumption **(E)** holds. Given a solution F of the SSWE (2), the following statements are equivalent:

(1) Assumption **(FP)** holds.
(2) Boundary condition (5) holds.

Assumptions **(E)** and **(FP)** also have important implications for the field at the interface of the fibre structure and the surrounding environment.

Theorem 2.5. Fix $l \in \mathbf{Z}$, $\beta, n_e \in \mathbf{R}_{\geq 0}$ and suppose that assumption **(E)** holds. Let F be a solution of the SSWE (2). Then, the following statements are equivalent:

(1) Assumption **(FP)** holds.
(2) F is of the form

$$F(s) \ = \ C_{l,\beta,n_e} K_l(W_{\beta,n_e}\, s). \tag{14}$$

for all $s \geq 1$.

(3) F satisfies the fibre / environment interface boundary condition given by

$$\frac{dF}{ds}(1) \ = \ \gamma_{l,\beta,n_e} F(1), \tag{15}$$

where $\gamma_{l,\beta,n_e} \in \mathbf{R}$ is a constant.

2.6 Normalized evanescent field power (NEFP)

Given a solution of the boundary value problem (1), (2), (3), (4), the unnormalized evanescent field power is the total power $\hat{P}(1,\infty;\psi)$, $\psi(s,\phi) := F_{l,\beta,n}(s)\Phi_l(\phi)$, in the field outside the fibre ($s \geq 1$). The normalized evanescent field power $\rho(\psi)$ is then defined by

$$\begin{aligned} \rho(\psi) := \frac{\hat{P}(1,\infty;\psi)}{\hat{P}(0,\infty;\psi)} &= \frac{P(1,\infty;F_{l,\beta,n}) \cdot Q_l(\Phi_l)}{P(0,\infty;F_{l,\beta,n}) \cdot Q_l(\Phi_l)} \\ &= \frac{P(1,\infty;F_{l,\beta,n})}{P(0,\infty;F_{l,\beta,n})}. \end{aligned} \tag{16}$$

As $\rho(\psi)$ is independent of the angular component Φ_l of the transverse electric field, we will occasionally abuse notation by writing $\rho(\psi) = \rho(F_{l,\beta,n}, \Phi_l) = \rho(F_{l,\beta,n})$.

Theorem 2.6. Where defined by (16), the normalized evanescent field power operator ρ is invariant with respect to scalar multiplication. That is, given fixed l, β, $n \in \mathcal{N}[0,\infty)$ and a solution $\psi(\cdot)$ to the boundary value problem (1), (2), (3), (4), (5), $\eta\psi(\cdot)$ is a solution to the same boundary value problem and satisfies $\rho(\eta\psi) = \rho(\psi)$ for all $\eta \in \mathbf{R}$.

3. NEFP MAXIMIZATION

3.1 Formulation

The main idea here is to maximize the field power that interacts with the environment outside the fibre structure. The is formalized in view of assumption **(E)**. Note that assumptions **(FD)** and **(FP)** will be a direct consequence of the specified constraints.

Problem (P1): Given the modal parameter l, the group velocity β and the environment RIP of assumption **(E)**, determine the maximizing RIP $n \in \mathcal{N}_\infty[0,1)$ for the normalized evanescent field power $\rho(F_{l,\beta,n})$, subject to the ODE constraint (2) and the boundary constraints (4) and (5).

3.2 Separation principle

Problem **(P1)** can be simplified via separation into a constrained power minimization problem for the field confined inside the fibre structure, and a direct integration to yield the evanescent

field power (outside the fibre structure). The fields inside and outside the fibre structure are then linked through the boundary condition (9), and when augmented, form a solution to the SSWE (2) with boundary conditions (4) and (5).

Problem (SPC): Given the modal parameter l, the group velocity β, and any boundary condition $x^1 \in \mathbf{R}^2$ for (9), determine the minimizing RIP $n_{x^1} \in \mathcal{N}_\infty[0,1)$ for the confined field power $P(0,1;F_{l,\beta,n})$ subject to the ODE constraint (2), and the boundary conditions (4) and (9). Formally, determine the value (left-hand side) and the corresponding minimizer for

$$\Pi^C_{l,\beta}(x^1) = \inf_{n\in\mathcal{N}[0,1)} \left\{ P(0,1;F_{l,\beta,n}) \,\middle|\, \begin{array}{l} F_{l,\beta,n} \\ \text{satisfies} \\ (2),\ (4),\ (9) \end{array} \right\} \tag{17}$$

Problem (SPE): Given the modal parameter l, the group velocity β, any boundary condition $x^1 \in \mathbf{R}^2$ for (9), and the environment RIP of assumption **(E)**, determine the evanescent field power $P(1,\infty;F_{l,\beta,n_e})$ subject to the ODE constraint (2), the boundary constraints (5) and (9). Formally, determine the value

$$\Pi^E_{l,\beta}(x^1) = P(1,\infty;F_{l,\beta,n_e}) \,\Big|\, \begin{array}{l} F_{l,\beta,n_e} \text{ satisfies} \\ (2),\ (5) \text{ and } (9) \end{array} \tag{18}$$

Problem (P2): Find the RIP $n^* \in \mathcal{N}[0,1)$ such that $n^* \equiv n_{x^{1*}}$, where $n_{x^{1*}}$ solves problem **(SPC)** and $x^{1*} \in \mathbf{R}^2$ is the minimizing x^1 for $\Pi^C_{l,\beta}(x^1)$ subject to the normalization constraint

$$\Pi^C_{l,\beta}(x^1) + \Pi^E_{l,\beta}(x^1) = 1, \tag{19}$$

where $\Pi^E_{l,\beta}(x^1)$ solves problem **(SPE)**.

Lemma 3.1. Given any $\eta \in \mathbf{R}$ and $\bullet \in \{C, E\}$, the value function $\Pi^\bullet_{l,\beta} : \mathbf{R}^2 \to \mathbf{R}_{\geq 0}$ satisfies

$$\Pi^\bullet_{l,\beta}(\eta x) \;=\; \eta^2 \Pi^\bullet_{l,\beta}(x) \tag{20}$$

for all $x \in \mathbf{R}^2$.

The separation principle can then be stated as follow.

Theorem 3.2. Problems **(P1)** and **(P2)** are equivalent.

3.3 Recipe

Problem **(P2)** and Theorem 3.2 present the evanescent field power maximization problem **(P1)** in a form that is amenable to solution via the simpler problems **(SPC)** and **(SPE)** and the normalization condition (19). Problems **(SPC)** can be addressed via dynamic programming (Bellman, 1957) and finite difference methods (Kushner and Dupuis, 1992), whilst problem **(SPE)** can be addressed via direct integration of Bessel function solutions. This motivates the following recipe, described by problem **(P2)** and applicable under assumptions **(FD)** and **(E)**, for solving the evanescent field power maximization problem **(P1)**:

(1) Fix the refractive index class $\mathcal{N}$, mode number $l \in \mathbf{Z}$ and propagation constant $\beta \in \mathbf{R}_{>0}$.
(2) Determine the fibre axis boundary conditions (4).
(3) Compute $\Pi^C_{l,\beta} : \mathbf{R}^2 \to \mathbf{R}$ and the corresponding optimizer via dynamic programming.
(4) Compute $\Pi^E_{l,\beta} : \mathbf{R}^2 \to \mathbf{R}$ via direct integration of solutions of SSWE (2).
(5) Determine the level set

$$\mathbf{X}_1 \;:=\; \left\{ x \in \mathbf{R}^n \,\middle|\, \Pi^C_{l,\beta}(x) + \Pi^E_{l,\beta}(x) = 1 \right\}. \tag{21}$$

(6) Determine the minimizer x^{1*} of $\Pi^C_{l,\beta}(x)$ on the level set $\mathbf{X}_1$, that is

$$x^{1*} \;:=\; \operatorname*{argmin}_{x\in\mathbf{X}_1} \Pi^C_{l,\beta}(x). \tag{22}$$

(7) Use the gradient of the function $\Pi^C_{l,\beta}$ to determine the optimal control (and hence the optimal refractive index) from x^{1*}.

Here, 3) solves problem **(SPC)**, 4) solves problem **(SPE)**, 5) applies the normalization (19), 6) finds the interface condition that maximizes the evanescent field power, and 7) delivers the optimal refractive index profile.

Remark 3.3. Steps 5) and 6) above can be simplified significantly through the application of Theorem 2.5. In particular, as the normalization (19) necessarily implies assumption **(FP)**, Theorem 2.5 states that we need only search over those interface conditions defined by the manifold (15). Typically, this involves considering only two elements of R^2.

3.4 Dynamic programming

Problem **(P2)** defines an optimal control problem over the radial interval $[0,1]$. In particular, $\Pi^C_{l,\beta}$ as given by (17) is the value function for a minimum energy control problem with boundary constraints (4) and (15).

As a first step towards computation, define a finite horizon version of (17), $\Pi^C_{l,\beta} : [0,1] \times [0,1] \times \mathbf{R}^2 \to \mathbf{R}_{\geq 0}$, as

$$\Pi^C_{l,\beta}(r,s,x_s) := \inf_{u\in\mathcal{U}[r,s)} \{J(r,s,x_s;u)\,|\,x(s)=x_s, \quad x(r) \text{ satisfies (4) } \} \tag{23}$$

where

$$J(r,s,x_s;u) := \int_r^s \sigma x'(\sigma) L x(\sigma)\, d\sigma,$$
$$L := \begin{bmatrix} 1 & 0 \\ 0 & 0 \end{bmatrix},$$
$$\mathcal{U}[r,s) := \{u \mid n \in \mathcal{N}[r,s),\ u \text{ defined by (8)}\}$$

with $x(\cdot)$ a solution of (7) for input $u \in \mathcal{U}[r,s)$.

The infinite horizon definition (17) of $\Pi^C_{l,\beta}(\cdot)$ can be recovered via the identity

$$\Pi^C_{l,\beta}(x) \;=\; \liminf_{r\downarrow 0} \Pi^C_{l,\beta}(r,1,x). \tag{24}$$

This can be used to compute $\Pi_{l,\beta}(\cdot)$ by first deriving a PDE representation of (23) via dynamic programming (Bellman, 1957). The dynamic programming principle (DPP) for (23) is presented in the following lemma, the proof of which is omitted.

Lemma 3.4. $\Pi^C_{l,\beta}$ as defined by (23) satisfies the following dynamic programming principle (DPP) for any $p \in [r,s)$:

$$\Pi^C_{l,\beta}(r,s,x_s) \;=\; \inf_{u\in U[p,s]} \left\{ \int_p^s \sigma x'(\sigma) L x(\sigma)\, d\sigma + \Pi^C_{l,\beta}(r,p,x(p)) \middle| x(s)=x_s \right\} \tag{25}$$

DPP (25) is an integral equation whose solution $\Pi^C_{l,\beta}$ may be nonsmooth and even discontinuous. However, utilizing notions of viscosity solutions (see for example (Elliot, 1987)), the incremental form of this integral equation can be defined. The proof of the following lemma is omitted.

Lemma 3.5. For any $r \le s \le 1$, $x \in \mathbf{R}^2$, the finite horizon value function $\Pi^C_{l,\beta}$ given by (23) is a viscosity solution of the PDE

$$0 \;=\; sx'Lx - \frac{\partial \Pi^C_{l,\beta}}{\partial s}(r,s,x) - \sup_{u\in\mathbf{U}} \left\{ \nabla_x \Pi^C_{l,\beta}(r,s,x)\cdot f(s,x,u) \right\} \tag{26}$$

subject to the boundary condition

$$\Pi^C_{l,\beta}(r,r,x) \;=\; \begin{cases} 0 & x \text{ satisfies (4) via (6)}, \\ \infty & \text{otherwise.} \end{cases} \tag{27}$$

Together, (23), (24) and Lemma 3.5 form the basis for completing step 3) in the recipe of the preceding section.

3.5 Numerical method

In order to compute the solution of PDE (26), an *implicit Markov chain approximation method* (IMCAM) was applied (Kushner and Dupuis, 1992). Essentially, the IMCAM is an iterative finite difference method that provides local consistency between the continuous dynamics of (7) and an approximating Markov chain defined on a grid of discrete states and positions. See (Kushner and Dupuis, 1992) for further details on this method.

4. APPLICATION

A tapered $5\,\mu m$ fibre sensor with prescribed refractive index limits of $n_{\min} = 1.456$ and $n_{\max} = 1.600$ is considered. The refractive index profile bounded by these limits is to be designed to achieve maximal evanescent field power, given a phase velocity of $10^7\,ms$ and a pump laser wavelength of $850\,nm$. In summary,

$$\begin{array}{rlrl} n_{\min} &= 1.456 & n_{\max} &= 1.600 \\ n_e &= 1.333 & n_{eff} &= 1.476 \\ R &= 5\,\mu m & \lambda &= 850\,nm \\ l &= 0 & \beta &= 1.091\times 10^7 \\ W_{l,\beta} &= 23.41 & \gamma_{l,\beta,n_e} &= -23.90 \\ \mathcal{N} &= \mathcal{N}_\infty & & \end{array} \tag{28}$$

Following the steps of the optimal refractive index profile RECIPE,

(1) See (28) above.
(2) $l = 0$ and (4) $\Rightarrow x(0) = \begin{bmatrix} F_{l,\beta,n}(0) \\ \dfrac{dF_{l,\beta,n}}{ds}(0) \end{bmatrix} = \begin{bmatrix} x_1 \\ 0 \end{bmatrix}$ for all $x_1 \in \mathbf{R}$.
(3) IMCAM yields the approximation shown in Figure 1.
(4) Direct integration of (14) yields $\Pi_{l,\beta,n_e}(\cdot)$. See Figure 2.
(5) The level set (21) consists of two points c_1 and c_2 obtained from Figure 2. Then, $\mathbf{X}_1 = \{c_1, c_2\}$.
(6) The minimizer (22) can (in this case) be either element in $\mathbf{X}_1$. Choose $x^{1*} = c_2$.
(7) Applying the optimal control obtained from IMCAM yields the optimal refractive index profile dependency $n^* \in \mathcal{N}[0,1)$ as shown in Figure 3. The optimal RIP can then be obtained from (8). The fraction of power in the evanescent field can also be determined to be approximately 15%.

REFERENCES

Agrawal, G.P. (2001). *Nonlinear fiber optics.* Academic Press. San Diego, CA, USA.

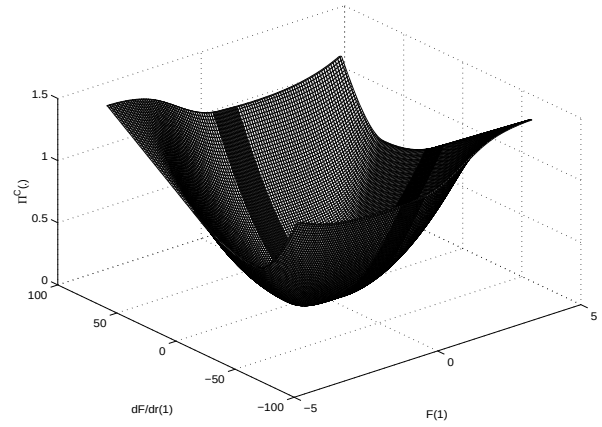

Fig. 1. Field power $\Pi^C_{l,\beta}(x)$ inside the optical fibre structure, $x \in \mathbf{R}^2$.

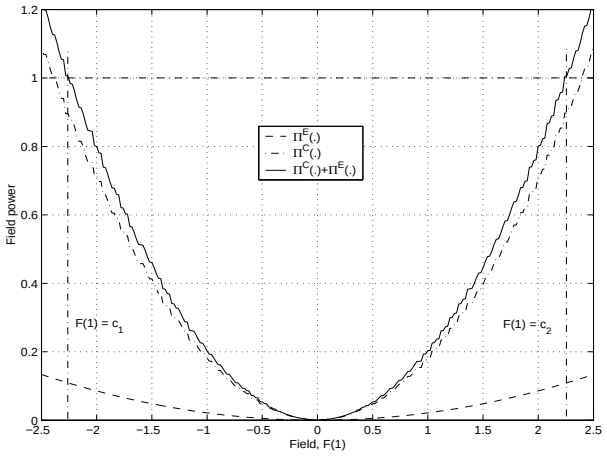

Fig. 2. Total field power $\Pi^C_{l,\beta}(x) + \Pi^E_{l,\beta}$, $x \in M_{l,\beta,n_e}$.

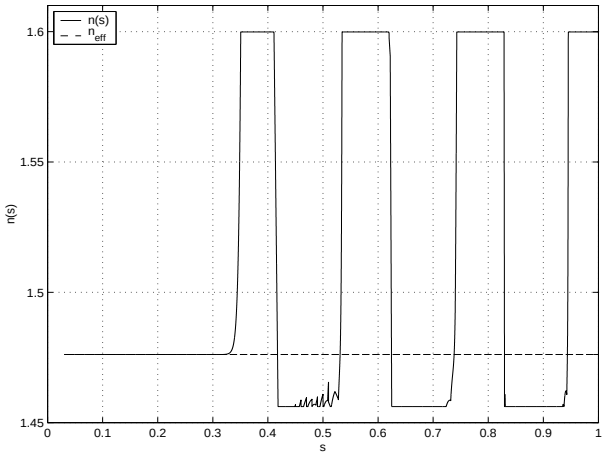

Fig. 3. Optimal refractive index profile.

Anderson, G. P., J. P. Golden, L. K. Cao, D. Wijesuriya, L. C. Shriver-Lake and F. S. Ligler (1994). Development of an evanescent wave fiber optic biosensor.. *IEEE Engineering in Medicine and Biology Magazine* **13**(3), 358–363.

Bellman, R. (1957). *Dynamic programming*. Princeton University Press. Princeton, NJ, USA.

Dower, P.M., P.M. Farrell and B.G. Gibson (2004). An optimal control problem arising in the design of optical fibre sensors. *To appear, Proc. 43rd IEEE Conference on Decision and Control (Bahamas)*.

Elliot, R.J. (1987). *Viscosity solutions and optimal control*. Pittman Research Notes in Mathematics Series, Wiley.

Gibson, B.C., J.D. Love, L.W. Cahill, P.M. Dower and D.M. Elton (2001). Evanescent field analysis of air-silica microstructure waveguides. *Proc. 14th Annual Meeting of the IEEE Lasers & Electro-Optics Society, LEOS (San Diego, USA)* **2**, 709–710.

Hale, Z. M. and F. P. Payne (1994). Fluorescent sensors based on tapered single-mode optical fibres. *Sensors and Actuators B* **17**(3), 233–240.

Helmers, H., P. Greco, R. Rustad, R. Kherrat, G. Bouvier and P. Benech (1996). Performance of a compact, hybrid optical evanescent-wave sensor for chemical and biological applications.. *Applied Optics* **35**(4), 676–680.

John, M. S., A. Kishen, L. C. Sing and A. Asundi (2002). Determination of bacterial activity by use of an evanescent-wave fiber-optic sensor.. *Applied Optics* **41**(34), 7334–7338.

Kumar, P. S., S. T. Lee, C. P. G. Vallabhan, V. P. N. Nampoori and P. Radhakrishnan (2002). Design and development of an led based fiber optic evanescent wave sensor for simultaneous detection of chromium and nitrite traces in water.. *Optics Communications* **214**(1-6), 25–30.

Kushner, H.J. and P.G. Dupuis (1992). *Numerical methods for stochastic control problems in continuous time*. Springer-Verlag.

Preejith, P. V., C. S. Lim, A. Kishen, M. S. John and A. Asundi (2003). Total protein measurement using a fiber-optic evanescent wave-based biosensor.. *Biotechnology Letters* **25**, 105–110.

Singh, C. D. and B. D. Gupta (1995). Detection of gases with porous-clad tapered fibers.. *Applied Optics* **34**(6), 1019–1023.

Snyder, A. and J.D. Love (1983). *Optical waveguide theory*. Chapman and Hall. London.

Sutherland, R. M., C. Dahne, J. F. Place and A. R. Ringrose (1984). Optical detection of antigen-antibody reactions at a glass-liquid interface.. *Clin. Chem.* **30**(9), 1533–1538.